tvst

Article

Assessment of Artifacts in Swept-Source Optical Coherence Tomography Angiography for Glaucomatous and Normal Eyes

Weijing Cheng[1], Yunhe Song[1], Fengbin Lin[1], Jian Xiong[1], Fei Li[1], Ling Jin[1], Zhenyu Wang[1], Chunman Yang[2], Bin Yang[3], Fanyin Wang[4], Guili Ning[5], Wei Wang[1], and Xiulan Zhang[1]

[1] State Key Laboratory of Ophthalmology, Zhongshan Ophthalmic Center, Sun Yat-Sen University, Guangzhou, China
[2] Department of Ophthalmology, The Second Affiliated Hospital of Guizhou Medical University, Guizhou, China
[3] Department of Ophthalmology, Zigong Third People's Hospital, Zigong, China
[4] Department of Ophthalmology, Shenzhen Qianhai Shekou Free Trade Zone Hospital, Shenzhen, China
[5] Department of Ophthalmology, Guizhou Aerospace Hospital, Zunyi, China

Correspondence: Xiulan Zhang, State Key Laboratory of Ophthalmology, Zhongshan Ophthalmic Center, Sun Yat-Sen University, No. 7 Jinsui Road, Guangzhou 510060, China.
e-mail: zhangxl2@mail.sysu.edu.cn

Received: July 25, 2021
Accepted: October 20, 2021
Published: January 18, 2022

Keywords: optical coherence tomography angiography; glaucoma; artifact; image quality

Citation: Cheng W, Song Y, Lin F, Xiong J, Li F, Jin L, Wang Z, Yang C, Yang B, Wang F, Ning G, Wang W, Zhang X. Assessment of artifacts in swept-source optical coherence tomography angiography for glaucomatous and normal eyes. Transl Vis Sci Technol. 2022;11(1):23, https://doi.org/10.1167/tvst.11.1.23

Purpose: To evaluate the frequency of and identify the factors that influence the artifacts of swept-source optical coherence tomography angiography (SS-OCTA) in glaucomatous and normal eyes.

Methods: Artifacts of OCTA images of open-angle glaucoma (OAG) and normal subjects were analyzed using SS-OCTA. Univariate and multivariate logistic regression analyses were performed to evaluate the association of age, sex, best-corrected visual acuity, axial length (AL), intraocular pressure, presence and severity of OAG, and image quality score (IQS) with the presence of artifacts.

Results: Images from 4426 subjects were included in the study. At least one type of artifact was present in 24.54% of the images. The most common artifacts were occurrence of motion (705 eyes, 15.93%), followed by defocus (628 eyes, 14.19%), decentration (134 eyes, 3.03%), masking (62 eyes,1.40%), and segmentation errors (23 eyes, 0.52%). Multivariate logistic analyses showed that the presence of OAG (odds ratio [OR] = 2.71; 95% confidence interval [CI], 2.09–3.51; $P < 0.001$), female sex (OR = 1.34; 95% CI, 1.12–1.61; $P = 0.001$), longer AL (OR = 1.09; 95% CI, 1.02–1.17; $P = 0.017$), and IQS < 40 (OR = 3.75; 95% CI, 3.15–4.48; $P < 0.001$) were significantly associated with higher odds for the presence of any artifact. The IQS had poor performance for detecting artifacts, with an area under the curve of 0.723, sensitivity of 73.04%, and specificity of 62.53%.

Conclusions: OAG eyes had more SS-OCTA image artifacts than normal eyes. IQS is an imperfect tool for identifying artifacts.

Translational Relevance: Special attention should be paid to the effect of artifacts when using SS-OCTA in the clinical setting to assess vascular parameters in patients with glaucoma.

Introduction

Optical coherence tomography (OCT) has fundamentally expanded our understanding of retinal and choroidal morphology and has become an essential tool for the diagnosis, monitoring, and management of glaucoma in clinical practice. The assessment of image artifacts is a key aspect of evaluating any new retinal imaging modality, because image artifacts can lead to incorrect diagnoses and errors in quantitative analysis.[1–7] Therefore, a variety of studies have been conducted to explore the frequency and associated factors of OCT image artifacts.[8–14]

Optical coherence tomography angiography (OCTA) is a non-invasive technique developed in

recent years to visualize the retinal and choroidal vasculature, which is considered a further extension of OCT technology. Recent studies have demonstrated that the value of OCTA parameters in the diagnosis and monitoring of glaucoma is not inferior to, or even better than, OCT parameters.[15–20] However, as with traditional OCT, image artifacts might seriously affect the measurements of OCTA images and its diagnostic efficacy for glaucoma.

Different types of artifacts in OCTA images have been described in recent studies, but the sample sizes of these studies were relatively small, and these studies mainly used spectral-domain (SD)-OCTA devices and focused on patients with retinal or choroidal lesions.[15] As pathological conditions change and OCT equipment varies, the frequency and severity of OCTA image artifacts change, and there are limited reports on the frequency of OCTA artifacts in glaucoma patients. To date, none of the studies, to the best of our knowledge, has explored the influencing factors associated with swept-source (SS)-OCTA artifacts in patients with glaucoma, which could help in subsequent optimization of software systems for artifact removal.

The aim of this study, therefore, was to investigate the frequency and distribution of image artifacts of SS-OCTA in glaucomatous and normal eyes, to identify its related factors, and to analyze the diagnostic efficacy of the image quality score (IQS) for image artifacts using the built-in software in the SS-OCTA device.

Materials and Methods

Participants

This retrospective observational study was approved by the Institutional Review Board of Zhongshan Ophthalmic Centre (ZOC), Sun Yat-sen University. The study was performed in accordance with the tenets of the Declaration of Helsinki. Signed, written, and informed consent was obtained from all subjects. All glaucomatous and healthy subjects presenting to the clinical research center of the ZOC were reviewed for eligibility for this study.

Normal eyes and eyes with open-angle glaucoma (OAG) were included in this study. The inclusion criteria for normal eyes were as follows: (1) eyes with open angles on gonioscopy; (2) eyes with best-corrected visual acuity (BCVA) $\geq$ 20/20; (3) eyes with intraocular pressure $\leq$ 21 mmHg measured using a Goldmann tonometer; (4) eyes without retinal nerve fiber layer (RNFL) defects on both OCT and fundus images; and (5) cup-to-disc ratio $\leq$ 0.3. The inclusion criteria for OAG eyes were as follows: (1) eyes with glaucomatous optic neuropathy; (2) eyes with typical glaucomatous visual field (VF) defects; and (3) gonioscopy demonstrating open angle.[21,22] The severity of glaucoma was categorized by mean deviation (MD) as mild ($-6 \leq$ MD ≤ 0), moderate ($-12 \leq$ MD ≤ -6), or advanced (MD ≤ -12).

Subjects presenting any of the following conditions were excluded from the study: (1) comorbidity with non-glaucomatous ocular diseases, such as uveitis, corneal opacity, cataracts, age-related macular degeneration, retinal artery occlusion, and diabetic retinopathy (DR); (2) non-glaucomatous optic neuropathy, such as a history of Parkinson's disease, Alzheimer's disease, optic neuritis, dementia, or stroke; and (3) eyes with a history of ocular trauma, intraocular surgery, or laser treatment.

Ocular Examination and SS-OCTA Imaging

All subjects underwent a complete ophthalmic examination, including slit-lamp biomicroscopy (BQ-900; Haag-Streit, Köniz, Switzerland); fundus photography with a stereoscopic fundus camera (Nonmyd WX-3D; Kowa Company, Nagoya, Japan); BCVA measurement with an Early Treatment Diabetic Retinopathy Study logMAR E chart (Precision Vision, Villa Park, IL); axial length (AL) measurement with optical coherence biometry (IOLMaster 500; Carl Zeiss Meditec, Jena, Germany); and VF testing using the Humphrey Field Analyzer with the 24-2 Swedish interactive threshold algorithm standard (Carl Zeiss Meditec). The VF report was checked for artifacts, including fatigue or learning effects, inattention, poor gaze, and eyelid or eyelash artifacts, and VF test results with such artifacts were excluded. A reliable VF report was defined as a fixation loss rate $\leq$ 33% and false-positive and false-negative error rates $\leq$ 15%.

A commercial SS-OCT instrument (DRI OCT-1 Triton; Topcon, Tokyo, Japan) was used for OCTA imaging. The unit had an acquisition rate of 100,000 A-scans per second operated at 1050-nm wavelength with an axial resolution of 8 µm. An eye-tracking system was used to reduce motion during OCTA imaging. OCTA scans were conducted in a 3 $\times$ 3-mm^2 region centered on the macula. The macular scans were divided into four slabs using automatic segmentation software: the superficial capillary plexus (SCP), deep capillary plexus, outer retina, and choriocapillaris. The SCP and B-scan images were selected for image quality assessment. Images were acquired in a dark room by an experienced technician. This SS-OCTA device provided an IQS using the built-in software (ImageNet 1.23), which ranged from 0 (poor)

to 100 (good). Based on the classification of IQS in most previous studies,[15,19,23] the IQS was classified into two categories: (1) 40 or above, and (2) below 40. If multiple OCTA images were acquired for one eye on the same day, only the eye with the highest IQS was used in this study.

Assessment of OCTA Image Artifacts and Image Processing

All SCP and B-scan images were assessed for the presence of artifacts by an OCT specialist and two trained graders, all of whom were blinded to the subject's disease status. This study classified image artifacts into five categories according to previous studies: motion, defocus, decentration, segmentation errors, and masking (Fig. 1). The definitions of these artifacts are detailed in Supplementary Table S1. According to the standard operating procedure (Supplementary Fig. S1), two graders performed an independent assessment of OCTA image artifacts while recording the type and number of each artifact, with the director of the clinical research center serving as the final arbitrator for any disagreement between the two graders.

Statistical Analysis

All statistical analyses were performed using SPSS Statistics 24 (IBM Corporation, Armonk, NY). Only data from the right eye were used in the analyses. Continuous data are expressed as mean ± standard deviation (SD) and categorical data as frequencies (percentages). Independent samples t-tests and χ^2 tests were used to evaluate the differences in demographics, clinical characteristics, and frequency of artifacts between subjects with glaucoma and normal controls. Univariate logistic regression was used to analyze the relationship between the presence of artifacts and relevant clinical factors such as age, BCVA, and disease status. For subjects with glaucoma, the relationship between the severity of visual field defects and artifacts was also analyzed. Multivariate logistic regression analysis was performed to determine the clinical variables that were independently associated with OCTA artifacts. Variables with $P < 0.10$, in univariate logistic regression, were included in multivariate logistic regression. Odds ratios (ORs) and 95% confidence intervals (CIs) were estimated. The IQS performance for detecting artifacts was assessed by the area under the curve (AUC) of a receiver operating characteristic (ROC) curve. $P < 0.05$, was considered indicative of a statistically significant difference.

Results

Demographic and Clinical Characteristics of the Included Subjects

A total of 4882 subjects underwent SS-OCTA examination, and 456 subjects were excluded from the study for the following reasons: non-glaucomatous ocular diseases ($n = 134$ eyes), non-glaucomatous optic neuropathy ($n = 105$ eyes), eyes with a history of surgery or trauma ($n = 86$ eyes), and unreliable VF report ($n = 131$ eyes). Finally, 4426 OCTA images from 4426 subjects were included in the present study. Table 1 shows the characteristics of the included subjects. The subjects had a mean age of 54.31 ± 15.69 years, and 53.78% were female. Subjects with glaucoma comprised 30.79% of the study population. On average, subjects with glaucoma were younger than the healthy controls (42.42 ± 15.22 years vs. 59.56 ± 12.76 years; $P < 0.001$) and demonstrated higher intraocular pressure, longer AL, and lower IQS ($P < 0.001$ for all).

Frequency and Distribution of OCTA Image Artifacts

Figure 2 shows the frequency of artifacts included in the present study. At least one type of artifact was present in 24.54% of the images. The most common artifacts were occurrence of motion in 705 eyes (15.93%), followed by defocus in 628 eyes (14.19%), decentration in 134 eyes (3.03%), masking in 62 eyes (1.40%), and segmentation errors in 23 eyes (0.52%).

The distribution of artifacts between groups is shown in Table 2. Glaucomatous eyes had a higher frequency of image artifacts than normal eyes (31.33% vs. 21.51%; $P < 0.001$). In particular, glaucomatous eyes were more likely to have defocus (21.35% vs. 11.00%; $P < 0.001$) and decentration (4.11% vs. 2.55%; $P = 0.005$) than the normal eyes. No statistically significant between-group differences were observed in the frequency of occurrence of motion (17.31% vs. 15.31%; $P = 0.461$), masking (1.61% vs. 1.31%, $P = 0.569$), or segmentation errors (0.37% vs. 0.59%; $P = 0.346$).

Factors Associated With the Occurrence of OCTA Image Artifacts

Table 3 presents the results of the logistic regression analyses for all the subjects. Multivariate logistic regression showed that glaucomatous eyes were more prone to image artifacts than normal eyes (OR = 2.71;

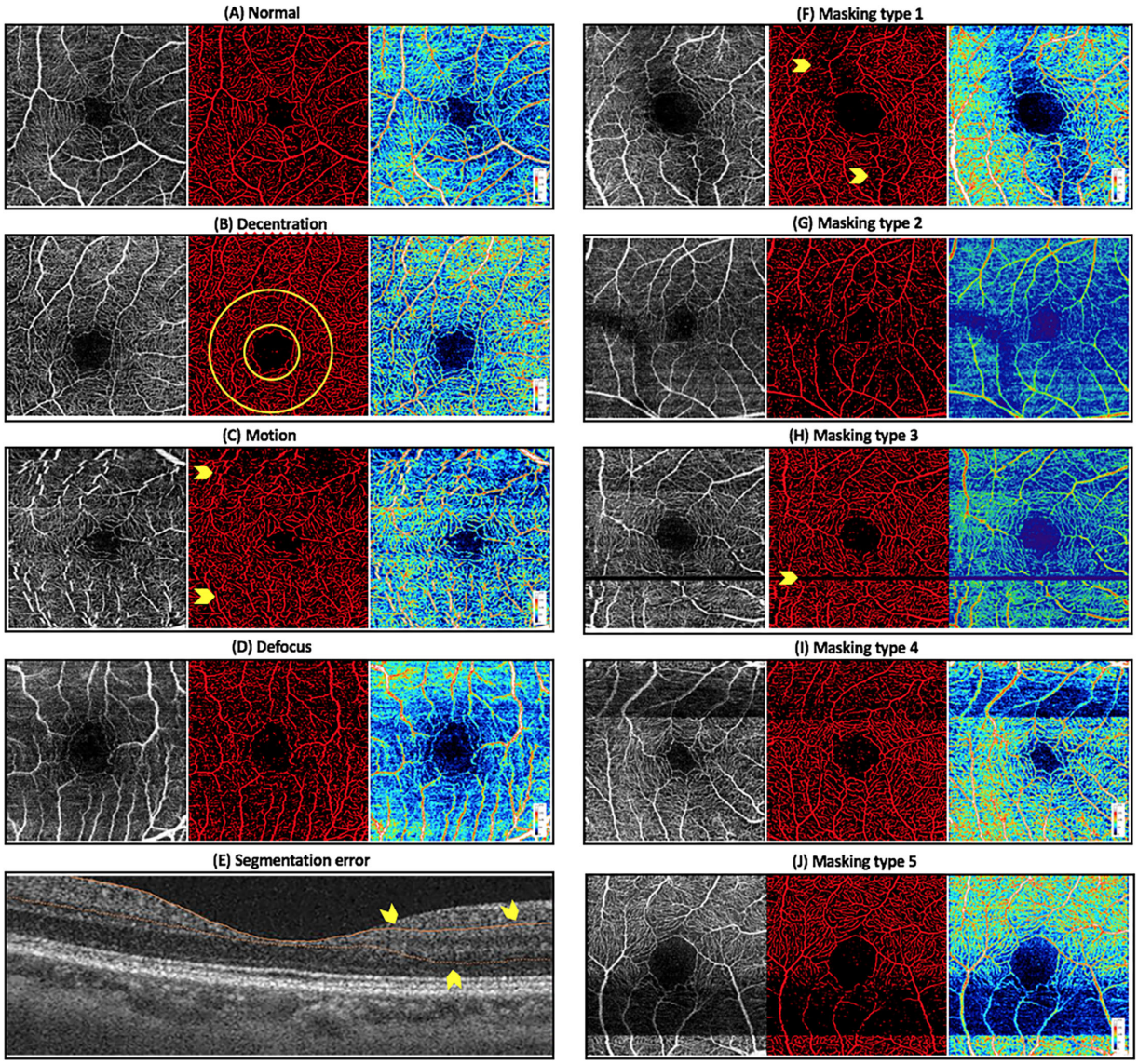

Figure 1. Examples of different types of scanning artifacts, both binarized and pseudo-color images in SS-OCTA imaging. (**A**) Normal image. Overall image quality and resolution were high without any artifacts. (**B**) Decentration. The foveal avascular zone region is off-center of the image, with partial vessels located outside the image. (**C**) Motion. Disruption of vascular signal with partial loss of microvascular signal (binary image, *yellow arrows*). (**D**) Defocus. Blurred macrovascular signal with severe loss of microvascular signal. (**E**) Segmentation errors. In the B-scan images, an error occurred in the internal limiting membrane/inner nuclear layer auto-stratification algorithm, and the corresponding en face vascular images are not at the same layer. *Hot colors* on the pseudo-color images are higher density. (**F**) Masking type 1. A vitreous floater obscures vessels, which results in irregular areas of partial microvascular signal loss (binary images, *yellow arrows*). (**G**) Masking type 2. Another type of irregular areas of partial microvascular signal loss. (**H**) Masking type 3. The patient blinks frequently, resulting in a loss of local horizontal linear signal loss that appears as horizontal black lines (binary images, *yellow arrows*). (**I**) Masking type 4. Inferior regular microvascular signal loss. (**J**) Masking type 5. Superior regular microvascular signal loss.

95% CI, 2.09–3.51; $P < 0.001$). Moreover, IQS < 40 was more likely to present with image artifacts (OR = 3.75; 95% CI, 3.15–4.48; $P < 0.001$). In the normal eyes, female sex (OR = 1.34; 95% CI, 1.12–1.61; $P < 0.001$) and longer AL (OR = 1.09; 95% CI, 1.02 – 1.17; $P = 0.017$) were associated with higher odds of image artifacts. Among glaucomatous eyes, advanced glaucoma (OR = 2.17; 95% CI = 1.02 –4.64; $P = 0.045$) was associated with the occurrence of image artifacts (Table 4).

Table 1. Demographic and Clinical Characteristics of Included Participants

Characteristic	Overall	Normal	Glaucoma	*P*[a]
No. of subjects (eyes)	4426 (4426)	3063 (3063)	1363 (1363)	—
Age (y), mean ± SD	54.31 ± 15.69	59.56 ± 12.76	42.42 ± 15.22	**<0.001**
Female gender, *n* (%)	2381 (53.78)	1979 (64.62)	402 (29.49)	**<0.001**
BCVA (logMAR), mean ± SD	0.16 ± 0.16	0.08 ± 0.15	0.09 ± 0.16	0.563
IOP (mmHg),[b] mean ± SD	15.76 ± 3.10	15.26 ± 3.66	15.90 ± 2.90	**<0.001**
AL (mm), mean ± SD	24.23 ± 1.64	23.77 ± 1.38	25.46 ± 1.65	**<0.001**
IQS, mean ± SD	55.59 ± 10.42	57.32 ± 11.26	51.65 ± 6.63	**<0.001**

IOP, intraocular pressure.
[a]*P* values are for comparisons between the normal group and the glaucoma group. Bold indicates statistical significance.
[b]All glaucoma eyes had been receiving multiple IOP-lowering eye drops.

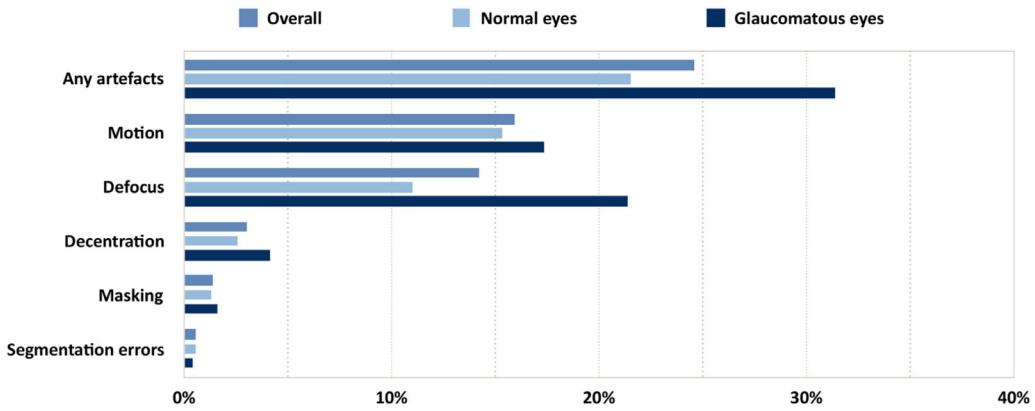

Figure 2. Frequency of the five types of artifacts in a total of 4426 scans from 4426 subjects using SS-OCTA.

Table 2. Prevalence of Artifacts Among the Normal and Glaucoma Eyes

Artifacts	Overall *n* (%)	Normal *n* (%)	Glaucoma *n* (%)	*P*[a]
Any artifacts	1086 (24.54)	659 (21.51)	427 (31.33)	**<0.001**
Motion	705 (15.93)	469 (15.31)	236 (17.31)	0.461
Defocus	628 (14.19)	337 (11.00)	291 (21.35)	**<0.001**
Decentration	134 (3.03)	78 (2.55)	56 (4.11)	**0.005**
Masking	62 (1.40)	40 (1.31)	22 (1.61)	0.569
Segmentation errors	23 (0.52)	18 (0.59)	5 (0.37)	0.346
Others	18 (0.41)	6 (0.20)	12 (0.88)	0.478

[a]*P* values are for comparisons between the normal group and the glaucoma group. Bold indicates statistical significance.

Diagnostic Performance of IQS for Detecting OCTA Image Artifacts

The mean AUC of the ROC curve of IQS for any type of artifact was only 0.723 (95% CI, 0.706–0.740), with a sensitivity of 73.04% and specificity of 62.53% (Fig. 3). Specifically, the AUC was 0.507 (95% CI, 0.448–0.566) for masking, 0.527 (95% CI, 0.476–0.579) for decentration, 0.616 (95% CI, 0.592–0.639) for occurrence of motion, 0.714 (95% CI, 0.695–0.733) for defocus, and 0.851 (95% CI, 0.758–0.942) for segmentation errors. Figure 4 shows examples of image artifacts but with IQS > 40.

Discussion

Artifacts are a common drawback of all imaging devices, especially for relatively new technologies such as OCTA. As OCTA becomes more widely used in clinical and research practice, it is important to

Table 3. Univariate and Multivariate Logistic Regression Analysis for Identifying Factors Associated With the Presence of Any Artifacts in All Subjects

	Univariate		Multivariate	
Factors	OR (95% CI)	*P*[a]	OR (95% CI)	*P*[a]
Age, per year	0.99 (0.99–0.99)	**<0.001**	1.00 (0.99–1.01)	0.504
Gender, female	0.97 (0.86–1.10)	0.660	—	—
IOP, per mmHg	0.97 (0.95–0.99)	**0.015**	0.99 (0.97–1.02)	0.591
IQS				
More than 40	Ref. (1.0)	—	Ref. (1.0)	—
Less than 40	3.87 (3.36–4.45)	**<0.001**	3.75 (3.15–4.48)	**<0.001**
BCVA, per logMAR	0.84 (0.42–1.31)	0.648	—	—
AL, per mm	1.24 (1.19–1.29)	**<0.001**	1.06 (1.00–1.13)	0.050
Presence of glaucoma	1.88 (1.65–2.14)	**<0.001**	2.71 (2.09–3.51)	**<0.001**

[a]Bold indicates statistical significance.

Table 4. Univariate and Multivariate Logistic Regression Analysis for the Presence of Any Artifacts in Subgroups of Glaucoma and Normal Subjects

	Univariate		Multivariate	
Factors	OR (95% CI)	*P*[a]	OR (95% CI)	*P*[a]
Normal subjects				
Age, per year	0.99 (0.99–1.00)	**0.002**	0.98 (0.96–0.99)	0.059
Gender, female	1.31 (1.12–1.52)	**0.001**	1.34 (1.12–1.61)	**0.001**
IOP, per mmHg	0.98 (0.95–1.00)	0.073	0.99 (0.96–1.02)	0.493
IQS				
More than 40	Ref. (1.0)	—	Ref. (1.0)	—
Less than 40	4.02 (3.39–4.78)	**<0.001**	3.74 (3.09–4.54)	**<0.001**
BCVA, per logMAR	0.77 (0.47–1.27)	0.308	—	—
AL, per mm	1.19 (1.13–1.26)	**<0.001**	1.09 (1.02–1.17)	**0.017**
Glaucoma subjects				
Age, per year	1.01 (1.01–1.02)	**<0.001**	0.99 (0.97–1.00)	0.163
Gender, female	1.01 (0.80, 1.28)	0.918	—	—
IOP, per mmHg	1.01 (0.97, 1.06)	0.553	—	—
IQS				
More than 40	Ref. (1.0)	—	Ref. (1.0)	—
Less than 40	3.21 (2.51–4.12)	**<0.001**	2.84 (1.82–4.43)	**<0.001**
BCVA, per logMAR	0.97 (0.67–1.37)	0.308	—	—
AL, per mm	1.07 (0.99–1.15)	0.0715	0.92 (0.80–1.06)	0.238
Stage of glaucoma				
Mild	Ref. (1.0)	—	Ref. (1.0)	—
Moderate	1.73 (1.23–2.43)	**0.002**	1.59 (0.94–2.69)	0.084
Advanced	4.20 (2.73–6.47)	**<0.001**	2.17 (1.02–4.64)	**0.045**

[a]Bold indicates statistical significance.

identify the frequency, type, and risk factors of artifacts. A better understanding of OCTA artifacts may also help to reduce their occurrence and allow the development of methods to reduce their impact on quantitative analysis. This study documented a high frequency of image artifacts in SS-OCTA and that the artifacts appeared more frequently in subjects with glaucoma than in normal subjects. The frequency of artifacts increased with increasing glaucoma severity. The presence of artifacts was also independently

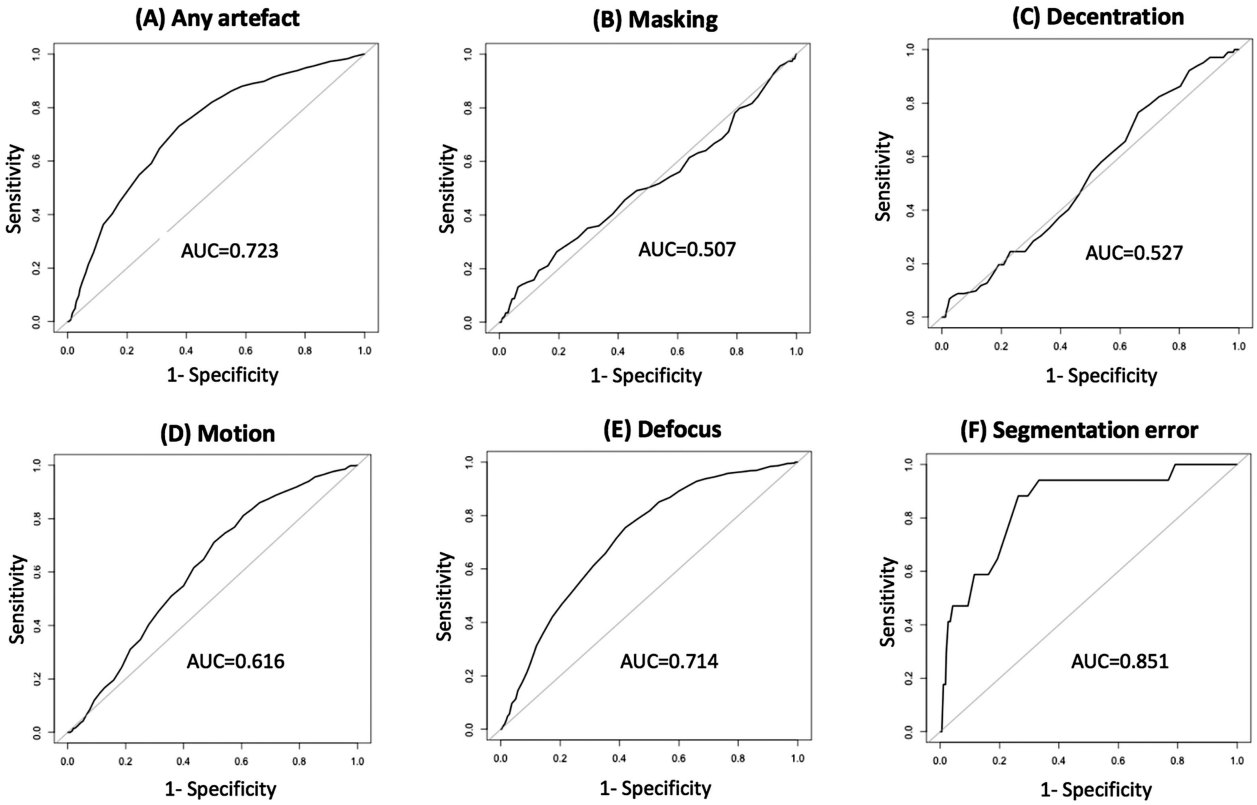

Figure 3. The ROC curves of IQSs for diagnosing any artifacts and each specific artifact. The diagnostic performance for (**A**) any artifact (AUC = 0.723); (**B**) masking (AUC = 0.507); (**C**) decentration (AUC = 0.527); (**D**) motion (AUC = 0.616); (**E**) defocus (AUC = 0.714); and (**F**) segmentation errors (AUC = 0.851). ILM, inner limiting membrane; IPL, inner plexiform layer; INL, inner nuclear layer.

associated with lower IQS, long AL, and female sex. Furthermore, the built-in IQS had limited diagnostic efficacy in identifying image artifacts, calling for a novel paradigm for identifying artifacts.

Only a few studies with small sample sizes have analyzed the distribution and related factors of OCTA image artifacts, which are summarized in Table 5. Iftikhar et al.[24] and Ghasemi et al.[25] found reported frequencies of artifacts of 93.1% and 58.33%, respectively. In patients with DR, Holmen et al.[26] found at least one artifact in 97.3% of images, with masking (26.9%), defocus (20.9%), and occurrence of motion (16.0%) being the three most common artifacts. This study found that the overall frequency of artifacts was 24.54%. We noticed a higher frequency of artifacts in the abovementioned studies, which may be related to the lack of rigorous training of technicians, the use of older versions of OCTA software, small sample size, and poor cooperation of patients.

Artifacts were more frequent in subjects with glaucoma than in normal controls, a finding consistent with previous studies on retinal and choroidal diseases. Only one study with a sample size of 28 eyes evaluated the frequency of OCTA image artifacts, and it reported that 35.7% of glaucomatous eyes had artifacts.[27] This study included 1363 glaucomatous eyes, further confirming that nearly one-third of glaucomatous eyes had OCTA image artifacts, especially defocus and decentration artifacts. Therefore, the impact of artifacts must be considered in the future clinical practice of glaucoma.

The most common artifacts found in this study were occurrence of motion (15.9%), defocus (14.2%), and decentration (3.0%). Previous studies have obtained similar findings, albeit in different order. Holmen et al.[26] found that, in patients with DR, masking (26.9%), defocus (20.9%), and occurrence of motion (16.0%) were the three most common types of artifacts. Enders et al.[28] found that among patients with DR, retinal artery occlusion, and age-related macular degeneration, projection artifacts (100.0%), segmentation errors (54.7%), and occurrence of motion (49.3%) were the three most common types of artifacts. Ifitikhar et al.[24] found that motion (96.3%), masking (51.9%), and decentration (25.1%) were the three most common types of artifacts in patients with multiple sclerosis. The difference in the frequency of artifact occurrence was mainly due to the inclu-

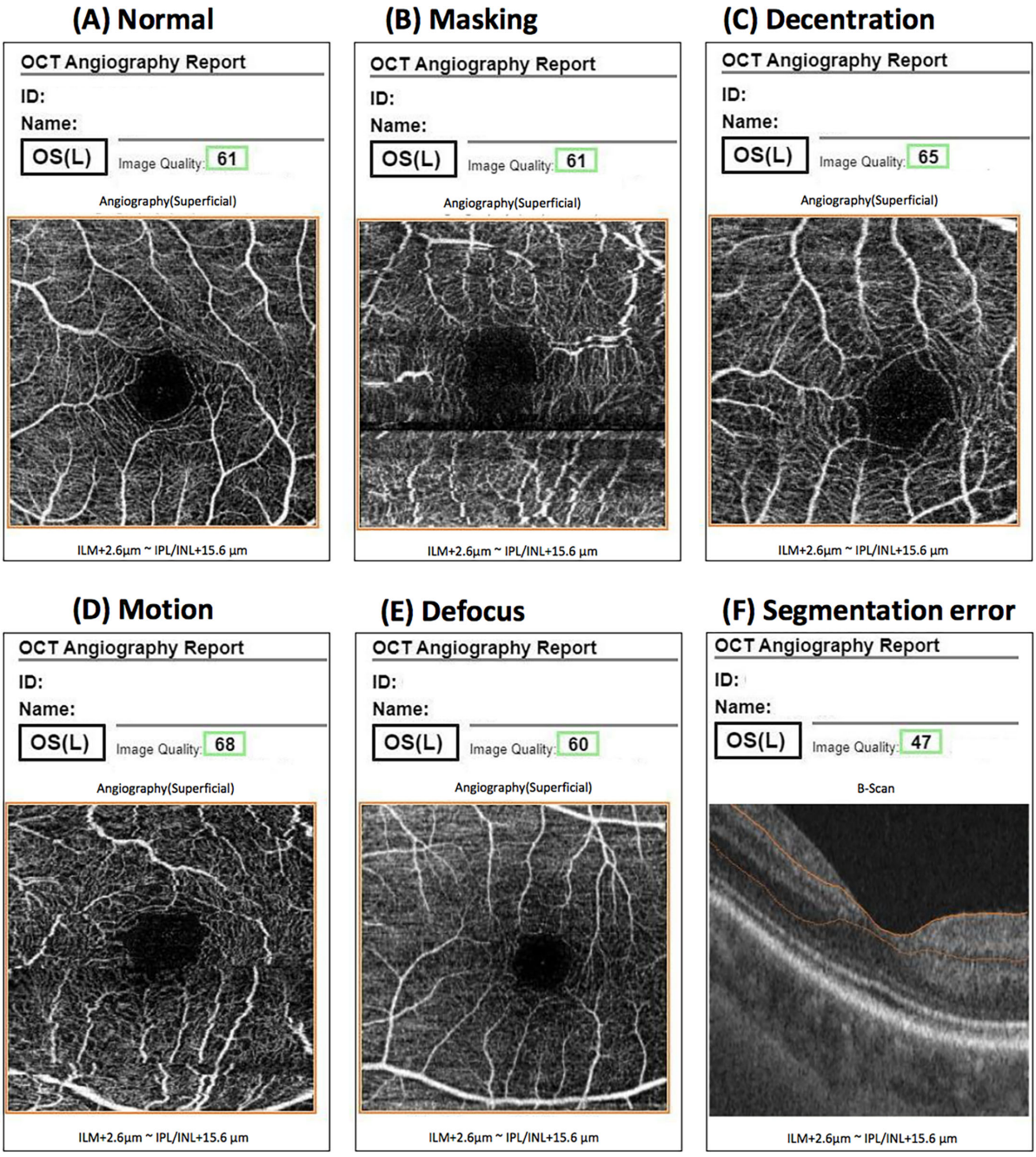

Figure 4. Example of the report of image quality for five typical artifacts. (**A**) High IQS without artifact. (**B**) High IQS with masking. (**C**) High IQS with decentration. (**D**) High IQS with motion. (**E**) High IQS with defocus. (**F**) High IQS with segmentation error.

sion of subjects with retinal diseases in a previous study. Although most of the current OCT instruments have eye-tracking options, the imaging principle of flow contrast in OCTA leads to inevitable motion. The occurrence of motion remains a major issue to be addressed in future OCTA imaging techniques.

In addition to glaucoma, the IQS and AL were also associated with the presence of artifacts. Few studies have evaluated factors associated with artifacts. Say et al.[29] found that, among patients with choroidal melanoma, the occurrence of artifacts was mainly associated with age, male sex, low visual acuity, plaque radiotherapy, and IQS. Cui et al.[30] found that, in patients with DR, the risk factors for OCTA image artifacts were the severity of DR and dry eyes. Iftikhar et al.[24] found that, in a multiple sclerosis population, the risk factors for OCTA image artifacts

Table 5. Previous Reports on the Frequency and Potential Factors Influencing the Presence of Artifacts in OCTA Imaging

Study	Subjects	Device	Eyes	Motion	Defocus	Decentration	Masking	Segmentation Errors	Influential Factors
Holmen et al.[26]	Retinal diseases	SD-OCTA	406	16.00%	20.90%	21.40%	26.90%	24.60%	NS
Cui et al.[30]	Retinal diseases	SS-OCTA	136	—	—	—	—	13.24%	NS
Enders et al.[28]	Retinal diseases	SD-OCTA	75	49.30%	—	9.30%	—	54.67%	NS
Iftikhar et al.[24]	MS and healthy	SD-OCTA	385	96.30%	—	25.10%	51.90%	—	Age, sex, visual acuity, MS, optic neuritis
Ghasemi et al.[25]	Retinal diseases	SS-OCTA	57	49.10%	—	1.70%	1.70%	61.40%	Presence of choroidal diseases
Lauermann et al.[36]	Retinal diseases	SD-OCTA	30	56.00%	—	—	38.30%	—	Lack of eye-tracking mode
Say et al.[29]	Retinal diseases	SD-OCTA	130	26.00%	—	55.00%	—	—	Radiotherapy, visual acuity, sex
Chen et al.[37]	Retinal diseases	SD-OCTA	60	70.00%	—	—	50.00%	—	NS
Present study	Glaucoma	SS-OCTA	1363	17.31%	21.35%	4.11%	1.61%	0.37%	IQS, severity
	Healthy		3063	15.31%	11.00%	2.55%	1.31%	0.59%	IQS, female, AL

NS, not studied; MS, multiple sclerosis.

were multiple sclerosis and history of optic neuritis. Woetzel et al.[27,31] and Alten et al.[32] found that OCTA image artifacts were associated with retinal and choroidal diseases. However, none of these studies included a sufficient sample of patients with glaucoma; therefore, our study further extends the previous research.

This study found that, among glaucomatous eyes, advanced glaucoma was associated with the occurrence of image artifacts (Table 4), which is in agreement with previous studies. Liu et al.[14] reported that advanced-stage glaucoma ($P < 0.001$) was associated with an increased prevalence of artifacts of the retinal nerve fiber layer in 2313 eye scans of 1188 patients who underwent a complete eye examination with OCT scanning from September 2009 to July 2013. The authors postulated that this finding may be due to glaucomatous RNFL thinning, which is associated with decreased RNFL reflectivity, leading to more algorithm failures. Similarly, it is now believed that patients with advanced glaucoma have more severe decreases in vessel density.[14] The decrease in glaucomatous vessel density is associated with decreased vessel reflectivity, which may also lead to more algorithm failures. This further suggests that clinicians should first assess scans for artifacts, before making therapeutic decisions based on OCT/OCTA measurements.

The diagnosis of open-angle glaucoma was associated with a higher prevalence of defocus artifacts compared with normal eyes. This may also be attributable to a decrease in vascular reflectivity, making automated vascular perfusion determinations more difficult, an observation that is in agreement with previous studies on OCT image artifacts. This study found no significant association between glaucoma and the increased frequency of motion artifact. However, few studies have explored this association yet. Glaucoma is a neurodegenerative disease with characteristic structural changes in the optic nerve and retinal nerve fiber layer.[16] Therefore, glaucoma does not affect eye movements, and glaucoma did not correlate with more motion artifacts.

The present study demonstrated that the IQS is an imperfect tool for discriminating between reliable and unreliable images, which is consistent with previous SD-OCTA studies. It has been reported that the IQS was not highly effective for the diagnosis of artifacts in Zeiss and Optovue (Fremont, CA) OCTA images (AUC = 0.80–0.83).[26] This study indicated that this problem also existed in the Topcon OCTA. For example, every IQS in Figure 4 was above 40, but there were clear image artifacts that should be excluded in image quality control. Therefore, future OCTA studies should incorporate quality control protocols when analyzing data from OCTA images. This may include a subjective assessment of all images to determine the presence and severity of different types of artifact. Recently, Lauermann et al.[33] proposed an artificial intelligence (AI)-based objective scoring scheme for OCTA image quality using the open-source digital library framework TensorFlow to build a convolutional neural network classifier that automatically evaluates OCTA image quality. The use of AI-assisted image quality control accelerates and facilitates the workflow of OCTA, contributes to reliable compliance with quality and analysis standards, and has a promising future in clinical applications.

A major strength of this study is its large sample size, with a total of 4426 subjects evaluated for OCTA images, making it the largest group to date. This study had several limitations. First, only one OCTA instrument was used. Caution is needed when generalizing our results to other brands of OCTA devices. We are currently studying the effects of different types of OCTA devices on artifacts. Second, this was a single-center study involving only Chinese subjects. Recent studies have reported a relationship between OCTA parameters and race.[34,35] The conclusions of this study should be taken cautiously when applied to other ethnicities. Third, only subjects with OAG

were included in this study, and subjects with other types of glaucoma, such as angle-closure glaucoma and secondary glaucoma, were not included. In the future, it will be necessary to investigate whether patients with other types of glaucoma have the same frequency of artifacts as in the present study. Fourth, only the major types of artifacts detailed in the literature were analyzed in this study; projection artifacts and some minor artifacts may be overlooked. However, the primary focus of this study was on analyzing artifacts that occur in the real world in a clinical setting, and the interpretation of OCTA images was mostly done through the SCP en face image and B-scans, so we chose to evaluate the five artifacts of interest rather than all types of artifacts. Fifth, our data are cross-sectional, and the study design prevented us from discerning causality; however, we believe that the large sample size of the database can provide valuable information. Furthermore, the retrospective nature of this study constitutes an inherent limitation, which may lead to selection bias. However, prospective studies are needed to validate the findings of this study. Finally, the current study analyzed only artifacts in the superficial layer and B-scan, and not in the other layers. This is because, in our clinical practice, the image quality of retinal blood flow is most commonly determined by the superficial layer; therefore, this is a reflection of a real clinical setting. In the future, further analysis of artifacts in other layers, including projection artifacts, will be necessary.

Conclusions

This large retrospective study demonstrated a higher frequency of artifacts in SS-OCTA images in subjects with glaucoma than in normal subjects, especially in subjects with an IQS of less than 40 and advanced glaucoma. The most common artifacts were occurrence of motion, defocus, and decentration. The IQS is an imperfect tool for identifying artifacts. These results indicate that stringent standardized image quality control should be implemented before further image analysis when using OCTA to assess glaucoma-related vascular parameters.

Acknowledgments

The authors thank all of the staff at the Zhongshan Ophthalmic Center. The data are available upon request. All data relating to this study were published. Any requests for data can be made to the corresponding author and subject to ethical approval.

Supported by the High-Level Hospital Construction Project, Zhongshan Ophthalmic Center, Sun Yat-sen University (303020104), and by the National Natural Science Foundation of China (82070955 and 82000901).

Disclosure: **W. Cheng**, None; **Y. Song**, None; **F. Lin**, None; **J. Xiong**, None; **F. Li**, None; **L. Jin**, None; **Z. Wang,** None; **C. Yang,** None; **B. Yang,** None; **F. Wang,** None; **G. Ning,** None; **W. Wang**, None; **X. Zhang**, None

References

1. Leung CK, Chan W, Chong KK, et al. Alignment artifacts in optical coherence tomography analyzed images. *Ophthalmology*. 2007;114:263–270.
2. Ho J, Sull AC, Vuong LN, Na JH, Kim HK, Sohn YH. Assessment of artifacts and reproducibility across spectral- and time-domain optical coherence tomography devices. *Ophthalmology*. 2009;116:1960–1970.
3. Hwang YH, Kim YY, Jin S, Na JH, Kim HK, Sohn YH. Errors in neuroretinal rim measurement by Cirrus high-definition optical coherence tomography in myopic eyes. *Br J Ophthalmol*. 2012;96:1386–1390.
4. Taibbi G, Peterson GC, Syed MF, Vizzeri G. Effect of motion artifacts and scan circle displacements on Cirrus HD-OCT retinal nerve fiber layer thickness measurements. *Invest Ophthalmol Vis Sci*. 2014;55:2251–2258.
5. Ye C, Yu M, Leung CK. Impact of segmentation errors and retinal blood vessels on retinal nerve fibre layer measurements using spectral-domain optical coherence tomography. *Acta Ophthalmol*. 2016;94:e211–e219.
6. Mansberger SL, Menda SA, Fortune BA, Gardiner SK, Demirel S. Automated segmentation errors when using optical coherence tomography to measure retinal nerve fiber layer thickness in glaucoma. *Am J Ophthalmol*. 2017;174:1–8.
7. Kong M, Eo DR, Han G, Park SY, Ham D-I. Error rate of automated choroidal segmentation using swept-source optical coherence tomography. *Acta Ophthalmol*. 2016;94:e427–e431.
8. Han IC, Jaffe GJ. Evaluation of artifacts associated with macular spectral-domain optical coherence tomography. *Ophthalmology*. 2010;117:1177–1189.

9. Hwang YH, Kim MK, Kim DW. Segmentation errors in macular ganglion cell analysis as determined by optical coherence tomography. *Ophthalmology*. 2016;123:950–958.
10. Asrani S, Essaid L, Alder BD, Santiago-Turla C. Artifacts in spectral-domain optical coherence tomography measurements in glaucoma. *JAMA Ophthalmol*. 2014;132:396–402.
11. Li A, Thompson AC, Asrani S. Impact of artifacts from optical coherence tomography retinal nerve fiber layer and macula scans on detection of glaucoma progression. *Am J Ophthalmol*. 2020;221:235–245.
12. Ray R, Stinnett SS, Jaffe GJ. Evaluation of image artifact produced by optical coherence tomography of retinal pathology. *Am J Ophthalmol*. 2005;139:18–29.
13. Mansouri K, Medeiros FA, Tatham AJ, Marchase N, Weinreb RN. Evaluation of retinal and choroidal thickness by Swept-Source optical coherence tomography: repeatability and assessment of artifacts. *Am J Ophthalmol*. 2014;157:1022–1032.
14. Liu Y, Simavli H, Que CJ, et al. Patient characteristics associated with artifacts in Spectralis optical coherence tomography imaging of the retinal nerve fiber layer in glaucoma. *Am J Ophthalmol*. 2015;159:565–576.
15. Liu L, Jia Y, Takusagawa HL, et al. Optical coherence tomography angiography of the peripapillary retina in glaucoma. *JAMA Ophthalmol*. 2015;133:1045.
16. Yarmohammadi A, Zangwill LM, Diniz-Filho A, et al. Relationship between optical coherence tomography angiography vessel density and severity of visual field loss in glaucoma. *Ophthalmology*. 2016;123:2498–2508.
17. Moghimi S, Hou H, Rao H, Weinreb RN. Optical coherence tomography angiography and glaucoma: a brief review. *Asia Pac J Ophthalmol (Phila)*. 2019;8:115–125.
18. Park HY, Shin DY, Jeon SJ, Park CK. Association between parapapillary choroidal vessel density measured with optical coherence tomography angiography and future visual field progression in patients with glaucoma. *JAMA Ophthalmol*. 2019;137:681–688.
19. Wan KH, Lam AKN, Leung CK. Optical coherence tomography angiography compared with optical coherence tomography macular measurements for detection of glaucoma. *JAMA Ophthalmol*. 2018;136:866–874.
20. Hou H, Moghimi S, Zangwill LM, et al. Macula vessel density and thickness in early primary open-angle glaucoma. *Am J Ophthalmol*. 2019;199:120–132.
21. Jonas JB, Aung T, Bourne RR, Bron AM, Ritch R, Panda-Jonas S. Glaucoma. *Lancet*. 2017;390:2183–2193.
22. Prum BJ, Rosenberg LF, Gedde SJ, et al. Primary Open-Angle Glaucoma Preferred Practice Pattern guidelines. *Ophthalmology*. 2016;123:P41–P111.
23. Sun Z, Tang F, Wong R, et al. OCT angiography metrics predict progression of diabetic retinopathy and development of diabetic macular edema. *Ophthalmology*. 2019;126:1675–1684.
24. Iftikhar M, Zafar S, Gonzalez N, et al. Image artifacts in optical coherence tomography angiography among patients with multiple sclerosis. *Curr Eye Res*. 2019;44:558–563.
25. Ghasemi Falavarjani K, Al-Sheikh M, Akil H, Sadda SR. Image artefacts in swept-source optical coherence tomography angiography. *Br J Ophthalmol*. 2017;101:564–568.
26. Holmen IC, Konda SM, Pak JW, et al. Prevalence and severity of artifacts in optical coherence tomographic angiograms. *JAMA Ophthalmol*. 2020;138:119–126.
27. Lauermann JL, Woetzel AK, Treder M, et al. Prevalences of segmentation errors and motion artifacts in OCT-angiography differ among retinal diseases. *Graefes Arch Clin Exp Ophthalmol*. 2018;256:1807–1816.
28. Enders C, Lang GE, Dreyhaupt J, Loidi M, Lang GK, Werner JU. Quantity and quality of image artifacts in optical coherence tomography angiography. *PLoS One*. 2019;14:e210505.
29. Say EAT, Ferenczy S, Magrath GN, Samara WA, Khoo CTL, Shields CL. Image quality and artifacts on optical coherence tomography angiography: comparison of pathologic and paired fellow eyes in 65 patients with unilateral choroidal melanoma treated with plaque radiotherapy. *Retina*. 2017;37:1660–1673.
30. Cui Y, Zhu Y, Wang JC, et al. Imaging artifacts and segmentation errors with wide-field swept-source optical coherence tomography angiography in diabetic retinopathy. *Transl Vis Sci Technol*. 2019;8:18.
31. Woetzel AK, Lauermann JL, Kreitz K, et al. Optical coherence tomography angiography image quality assessment at varying retinal expertise levels. *J Curr Ophthalmol*. 2019;31:161–167.
32. Alten F, Lauermann JL, Clemens CR, Heiduschka P, Eter N. Signal reduction in choriocapillaris and segmentation errors in spectral domain OCT angiography caused by soft drusen. *Graefes Arch Clin Exp Ophthalmol*. 2017;255:2347–2355.

33. Lauermann JL, Treder M, Alnawaiseh M, Clemens CR, Eter N, Alten F. Automated OCT angiography image quality assessment using a deep learning algorithm. *Graefes Arch Clin Exp Ophthalmol*. 2019;257:1641–1648.
34. Giocanti-Aurégan A, Gazeau G, Hrarat L, et al. Ethnic differences in normal retinal capillary density and foveal avascular zone measurements. *Int Ophthalmol*. 2020;40:3043–3048.
35. Wylęgała A, Wang L, Zhang S, Liu Z, Teper S, Wylęgała E. Comparison of foveal avascular zone and retinal vascular density in healthy Chinese and Caucasian adults. *Acta Ophthalmol*. 2019;98:e464–e469.
36. Lauermann JL, Treder M, Heiduschka P, Clemens CR, Eter N, Alten F. Impact of eye-tracking technology on OCT-angiography imaging quality in age-related macular degeneration. *Graefes Arch Clin Exp Ophthalmol*. 2017;255:1535–1542.
37. Chen FK, Viljoen RD, Bukowska DM. Classification of image artefacts in optical coherence tomography angiography of the choroid in macular diseases. *Clin Exp Ophthalmol.* 2016;44(5): 388–399.